Nonlin. Processes Geophys. Discuss., https://doi.org/10.5194/npg-2017-57
Manuscript under review for journal Nonlin. Processes Geophys.
Discussion started: 9 October 2017

Nonlinear Processes in Geophysics
Discussions
Open Access
EGU

Source site of internal solitary waves in the northern South China of westward shoaling thermocline

Gang Wang[1,2,3*], Yuanling Zhang[1,2,3], Chang Zhao[1,2], Dejun Dai[1,2,3], Min Zhang[1,2,3], Fangli Qiao[1,2]

[1]Key Laboratory of Data Analysis and Applications, the First Institute of Oceanography, State Oceanic Administration, Qingdao 266061, China
[2]Laboratory for Regional Oceanography and Numerical Modeling, Qingdao National Laboratory for Marine Science and Technology, Qingdao 266237, China
[3]Key Laboratory of Marine Science and Numerical Modeling (MASNUM), the First Institute of Oceanography, State Oceanic Administration, Qingdao 266061, China

Corresponding to： Gang Wang (wangg@fio.org.cn)

Abstract This study use a three dimensional general circulation model, MITgcm with non-hydrostatic option, to study the source site of internal solitary waves (ISWs) observed in the northern South China Sea. Simulation reveals that besides Luzon Strait, ISWs in the northern SCS are also generated around Dongsha Islands and near the continental shelf break. It is one of the reasons that there are more wave package to the west of 120oE in SAR images, and even more to the west of 118oE. The generation process and propagation feature of ISWs in these source sites are described.

1 Introduction

South China Sea (SCS), who connects the Pacific via Luzon Strait in its northeast (Figure 1(a)), is one of the largest marginal seas of the world oceans. Figure 1(b) sketches the topography of northern portion of the SCS, in which two meridional running ridges are parallel in Luzon Strait: Lanyu Ridge (the eastern ridge, which is also known as Luzon Island Arc) and Hengchun Ridge (the western one). The SCS is also characterized by large amplitude internal solitary waves (ISWs) ubiquitously in the sea basin. In field observations at the northern SCS, ISWs are recorded once or twice each day (Duda, 2004) during spring tide, propagating westward from Luzon Strait into the SCS (Liu and Hsu, 2004; Zhao et al., 2004; Fang and Du, 2005; Guo and Chen, 2012).The double-ridge configuration in Luzon Strait favors the generation of ISWs when tidal current from the Pacific flows through the strait into the SCS.

Nonlin. Processes Geophys. Discuss., https://doi.org/10.5194/npg-2017-57
Manuscript under review for journal Nonlin. Processes Geophys.
Discussion started: 9 October 2017

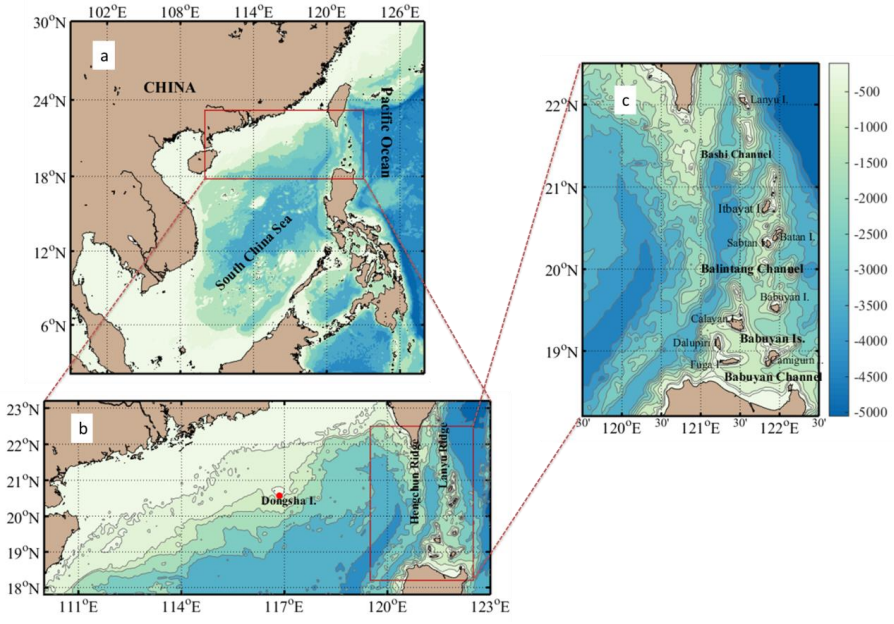

Figure 1: The bathymetry of the South China Sea.

Since the late 1970s, Synthetic Aperture Radars (SARs) have recorded thousands of ISWs all over the SCS. Statistics based on SAR images (Liu and Hsu, 2004, 2009; Zhao et al., 2004; Fang and Du, 2005; Gan et al., 2007; Yang et al., 2008; Farmer et al., 2009; Cai et al., 2012) profiles the spatial distribution of the ISWs in the SCS, in which wave crests concentrate in a band from Luzon Strait to Hainan Island. The ISWs occurred in this band are believed to be originated directly from, or closely related to the tidal current from the Pacific (Cai et al., 2002; Liu and Hsu, 2004; Zhao et al., 2004; Fang and Du, 2005; Lien et al., 2005; Gan et al., 2007; Jan et al., 2007; Wang et al., 2010; Cai et al., 2012).

In the last 20 years, in situ observations have been carried out intensively in the northern SCS to reveal the spatial and temporal features of ISWs beneath the sea surface. Cai et al. (2001) and Fang et al. (2005) reported a mooring observation in 1998 which recorded several ISWs of amplitude over 100 m near the Dongsha Island (20.70°N, 116.72°E). The largest amplitude of those waves reaches up to 160 m. During the Asian Seas International Acoustics Experiment (ASIAEX) undertaken in April and May 2001, twenty-one moorings deployed in the northeastern SCS recorded the shoaling of ISWs near the continental shelf break (Orr and Mignerey, 2003; Liu and Hsu, 2004: Ramp et al., 2004; Yang et al., 2004). Since 2005, observations related to the ISWs in the northern SCS increase noticeably (Yang et

Nonlin. Processes Geophys. Discuss., https://doi.org/10.5194/npg-2017-57
Manuscript under review for journal Nonlin. Processes Geophys.
Discussion started: 9 October 2017

al., 2009; Xu et al., 2010a, 2010b; Klymak et al., 2006; Tian et al., 2006; Li and Farmer, 2011; Alford et al., 2010; Liao et al., 2011; Si et al., 2010; Gao et al., 2010; Buijsman et al., 2012, 2014; Rainville et al., 2013; Li et al., 2014; Huang et al., 2014; Pickering& Alford, 2015; Dong et al., 2015). These observations reveal many details of spatial and temporal features on the ISWs in the northern SCS. Table 1 is a portion of the observations since 1998.

Table1: In situ observations on internal waves in the SCS since 1998

Reference	Observation Center	Time Span	Location
Cai, Gan et al., 2001 Fang, Shi et al., 2005 Orr et al., 2004;	Institute of Oceanology, CAS	1998.05-1998.06	116 °50.6'E; 20 °21.3'N
Liu, Hsu, 2004; Ramp et al., 2004; Yang et al., 2004	China, Kearo, Singapore et al., ASIAEX	Spring of 2000, spring of 2001	117-119 °E; 20-22.5 °N
Xu et al., 2010a, 2010b	Institute of Oceanology, CAS	2005.04- 2005.10	112 °E; 19 °35'N Wenchang station
Klymak et al., 2006	R/V Revelle	2005.04.15- 2005.05.15	119-120.5 °E; 20-21 °N
Yang et al., 2009	Taiwan/U.S, VANS/WISE	2005.04.29-2005.07.28 2005.11.02-2006.02.24	117°16.98'E; 21°36.87'N
Tian et al., 2006	Ocean University of China R/V	2005.10.04- 2005.10.16	Meridional Transect at 120.5 °E, Luzon Strait
Li, Farmer, 2011	unknown	2005, 2007	118.37-121.18 °E; 20.39-21.22 °N
Alford et al., 2010	Taiwan and U.S., NLIWI	2006.07-2007.05	116.5-121.8 °E; 20.6-21.1 °N
Rainville et al., 2013	ONR etc.	2007-	23,000 profiles from gliders near Luzon Strait
Liao et al., 2011	The Second Institute of Oceanography, SOA, China	2008.04.25; 2008.09.26	120°30.33'E; 20°59.96'N
Gao et al., 2010	Ocean University of China	2008.08.24- 2008.09.03	121 °E; 19.5-21 °N
Sun et al. 2015	SCOPE	2008.07.01-2008.07.17	115.6 °E, 22.0 °N
	CHOICE-C	2009.06-14-2008.07.07	116.66 °E,22.19 °N
Si et al., 2010	Institute of Oceanology, CAS	2009.06.24- 2009.06.25	117.5 °E; 21 °N, northeast to Dongsha Island
Li Zimu et al., 2014	South China Sea Institute of Oceanology, CAS	2010.09.04-2011.09.04	119°51'E; 20°33'N
Huang et al., 2014	unknown	2010.03-2010.08	119.1 °E; 21.1 °N
Pickering, Alford, 2015	unknown	2011	121°40.5'E; 20°31.4'N 121°1.8'E; 19°18'N
Dong et al., 2015	Ocean University of China	2012.10.02- 2012.10.04	118°24.62'E; 20°59.91'N

Nonlin. Processes Geophys. Discuss., https://doi.org/10.5194/npg-2017-57
Manuscript under review for journal Nonlin. Processes Geophys.
Discussion started: 9 October 2017

In the recent 10 years, primitive equation ocean models become popular in investigating the generation and propagation of both the ISWs and internal tides in the SCS (Table 2). Those models include hydrostatic models such as ONFS (Chao et al., 2007), DieCAST (Du et al., 2008) and POM (Jan et al, 2008); quasi-hydrostatic models such as HAMSOM (Song et al., 2010); and non-hydrostatic models such as HAMSOM (Li Huang et al., 2011), ROMS (Buijsman et al., 2010b) and MITgcm (MIT general circulation model, Marshall et al., 1997). Among these models the favorite one is probably the non-hydrostatic MITgcm (Vlasenko et al., 2010; Wang et al., 2010; Li et al., 2011; Guo et al., 2011; Guo et al., 2012; Vlasenko et al., 2012; Li Dan et al., 2012; Alfort et al., 2015; Wang et al., 2015; Wang et al., 2016), which takes upon around half of the simulations that we listed in Table 2.

Table 2: The simulations on internal waves in the SCS using primitive equation ocean models

Reference	Model	Nonhydrostatic	Initial T/S field	Model coverage
Chao et al., 2007	ONFS	No	unknown	116-123 ℃, 17-23.5 ℃
Du et al., 2008	DieCAST	No	*H-uniform, 2D	118-122 ℃
Jan et al, 2008	POM	No	H-uniform	99.25-135.25 ℃, 2.25-43.25 ℃
Warn-Varnas et al, 2010	unknown	Yes	NCOM, 2D	117-123 ℃
Buijsman et al, 2010	ROMS	Yes	H-uniform, 2D	20.58 ℃ , 117-126 ℃
Song et al., 2010	HAMSOM	Quasi	2D	20 ℃ , 115-130 ℃
Li & Song et al., 2011	HAMSOM	Yes	SODA 3D	16-23 ℃, 110-125 ℃
Zhang et al., 2011	SUNTANS	yes	H-uniform	18-23 ℃, 115-124 ℃
Vlasenko et al., 2010	MITgcm	Yes	H-uniform	20-21 ℃, 118-122.5 ℃
Wang et al., 2010	MITgcm	Yes	H-uniform, 2D	20 ℃ , 118.5-123 ℃
Li & Chen et al., 2011	MITgcm	Yes	H-uniform, 2D	16-16.3 ℃, 110-118 ℃
Guo et al., 2011	MITgcm	Yes	H-uniform, 2D	20-21.2 ℃, 117-123 ℃
Vlasenko et al., 2012	MITgcm	Yes	H-uniform, 2D	20.25-20.75 ℃, 117-123 ℃
Guo and Chen, 2012	MITgcm	Yes	H-uniform	20-21 ℃, 118-122.5 ℃
Li et al., 2012	MITgcm	Yes	H-uniform	16-26 ℃, 110-126 ℃
Alfort et al., 2011	Hallberg Isopycnal model	unknown	H-uniform	17-25 ℃, 115-127.5 ℃
Jan et al., 2012	POM	No	H-uniform	18-23 ℃, 116.75-126.75 ℃
Buijsman et al., 2012	MITgcm	Yes	H-uniform, 2D	20.6 ℃ , 120.25-122.25 ℃
Wang, 2012	POM	No	SODA 3D	16-23 ℃ , 105.5-126 ℃
BLK et al., 2013	unknown	unknown	2D	unknown
Buijsman et al., 2014	MITgcm	Yes	H-uniform	Entire Luzon Strait
Pickering et al., 2015	MITgcm,	Yes	H-uniform	Entire Luzon Strait
	LZS	No		Entire East Asian seas
Alfort et al., 2015	MITgcm	Yes	H-uniform	18-24 ℃, 118-123 ℃

Wang et al., 2015	MITgcm	Yes	H-uniform	18.5-22.5 °N, 114.5-124.5 °E 18.5-22 °N, 116.2-123 °E
Wang et al., 2016	MITgcm	Yes	H-uniform	1.5-29.5 °N, 98.5-128.5 °E

*H-uniform stands for horizontally uniform

Based on the observations (SAR images or field data), several mechanisms for the generation of the ISWs in the northern SCS have been proposed. Tidal current from the Pacific (Hsu and Liu, 2000; Zhao et al., 2004; Lien, 2005; Zhang et al., 2005; Fang et al., 2005; Zheng et al., 2008; Du et al., 2008), lee waves to the west slope of the ridges (Warn-Varnas et al., 2010; Pinkel et al., 2012), Kuroshio (Hsu, 2000; Cai, 2003; Liu and Hsu, 2004; Yuan et al., 2006), and locally interacting nonlinear waves near the thermocline (Zhao et al., 2004) are all possible candidates for triggering the ISWs. Besides observation (SAR images and field experiments), numerical model is an important complementary tool in studying the ISWs in the SCS. However, there are still many observed features of ISWs that have not been explained by numerical simulation. For instance, simulation has not yet demonstrated how the A waves (ISW packets rank-ordered with a large leading wave and some smaller followed) or B waves (wave packets consisted of one single ISW) on northern shelf of the SCS are related to the tidal current from the Pacific.

We noticed that all of the simulations using MITgcm listed in Table 2 start from a horizontally homogenous density field, i.e., neglecting the spatial non-uniformity of stratification in the initial fields but extending the temperature and salinity profiles at a point to the whole model domain. This approach may cause bias for the numerical model to describe the generation and evolution of NIWs. For instance, Zheng et al. (2007) discussed that the thermocline shoaling in the SCS forces the growth of ISWs. In numerical experiments made by Buijsman et al. (2010), the westward shoaling of thermocline makes the eastward solitons be 28% smaller than those westward. Besides, shoaling pattern of the thermocline favors the growth of solitons. In this work, we set up an internal wave model with three dimensional initial temperature and salinity climatology fields derived from WOA2013 (World Ocean Atlas 2013, Locarnini et al., 2013; Zweng et al., 2013) as initial state, and study the source site of the ISWs in the SCS based on numerical experiments.

Nonlin. Processes Geophys. Discuss., https://doi.org/10.5194/npg-2017-57
Manuscript under review for journal Nonlin. Processes Geophys.
Discussion started: 9 October 2017

2 Model configurations

A non-hydrostatic MITgcm code is set up to study the temporal and spatial features of ISWs in the northern SCS. Compared with the simulations using MITgcm listed in Table 2, the current experiment is distinctive in that the initial temperature and salinity fields are horizontally non-uniformly (Fig. 2). This configuration makes the model more sensitive to the viscosity coefficient and temperature/salinity diffusion coefficients since horizontal advection or diffusion also involves in the vertical processes.

The topography used in this work is the 1 arc-minute global relief model, ETOPO1 (Smith et al., 1997; Amante and Eakins, 2011). And the internal wave model domain ranges from 110°E to 123°E in longitude and 18°N to 22.5°N in latitude, covers the whole Luzon Strait, as in Fig.1(b) enclosed. Zonal range from 110°E to 123°E is divided into 6000 grids with 210-m resolution. Meridional span of 4.5 arc degree is divided into 800 grids with resolution of 620 m. The water column are divided into 60 z-coordinate layers, 5-to-10-m resolution in the upper 200 m, less than 30 m in the upper 440 m, and then increases at a rate of about 1.2-fold until he maximum thickness of 700 m at the bottom layer. The maximum water depth is set to 5086 m. At each of the three (east, north and south) open boundaries, 13 sponge layers covering 1.2 arc-degrees are set to relax the waves from reflecting. Their thickness increased proportionally from innermost layer with normal grid to 40 km at the outermost boundary layer. Table 3 lists the domain parameters, model resolutions, and the data source for the topography, temperature/salinity field and external forcing.

Table 3 Setups of the numerical model

Topography	Initial T/S	Forcing current	Model domain	Resolution		
				x	y	z
ETOPO1	WOA2013 Summer	TPXO7.1 11 components	110-123 ℉; 18 -22.5 ℕ	~210 m, 6000 grids	~620 m, 800 grids	60 layers

The initial temperature and salinity fields are derived from WOA2013. And we interpolate the three dimensional climatological temperature and salinity in summer (JJA) into model grids.

The isotherm cross each meridional section shows a westward shoaling pattern. Meanwhile, a subsurface tongue of high salinity centers at about 300 m depth intruding westward from Luzon Strait.

Nonlin. Processes Geophys. Discuss., https://doi.org/10.5194/npg-2017-57
Manuscript under review for journal Nonlin. Processes Geophys.
Discussion started: 9 October 2017

117 As a result, the isopycnic presents a westward shoaling trend. The vertical density gradient reaching
118 maximum 90 m depth around 120°E and less than 50 m over the continental shelf.

119 Tidal current with 11 constituents (M2, S2, N2, K2, K1, O1, P1, Q1, MF, MM, M4) is derived from
120 TPXO7.1 (Egbert and Erofeeva, 2002) to force the model from the open boundaries. The running starts
121 from July 13, 2015, lasted one week. Figure 2 is the tidal current along the eastern boundary (123°E) of
122 the model in the first four days of the simulation. Diurnal current is dominant while the semi-diurnal
123 component is less important. Meridional tidal current is stranger than zonal component, and in tidal
124 current in northern portion is stronger than southern portion.

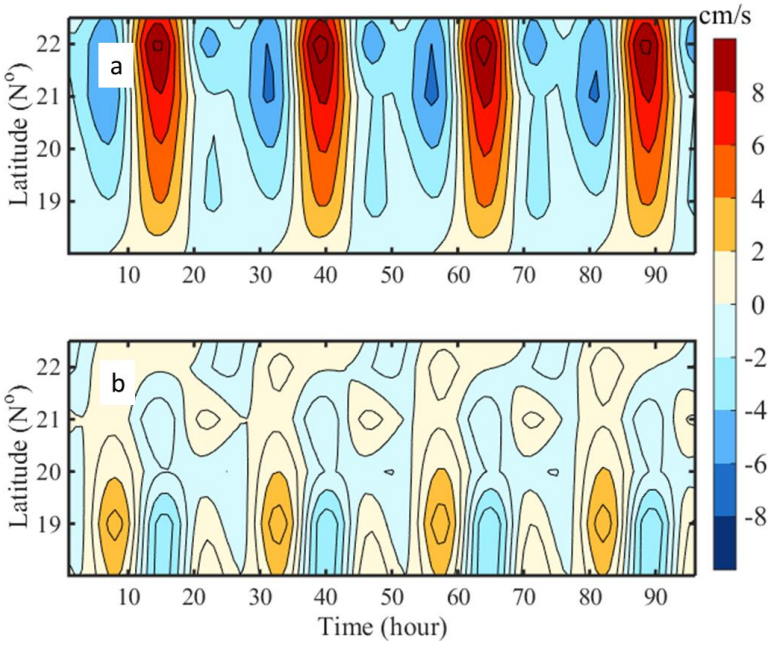

125

126 **Figure 2: Tidal current at the eastern boundary in the first four days of the simulation, (a) eastward current**
127 **(positive to the Pacific) and (b) northward current.**

128

129 **3 Simulation and Discussion**

130 The roughness of sea surface derived from surface current (u,v) is a widely used approach to inverse
131 the internal wave's signature, i.e.,

132 $$G = \sqrt{(\frac{\partial u}{\partial x})^2 + (\frac{\partial v}{\partial y})^2} \quad (1)$$

Nonlin. Processes Geophys. Discuss., https://doi.org/10.5194/npg-2017-57
Manuscript under review for journal Nonlin. Processes Geophys.
Discussion started: 9 October 2017

Nonlinear Processes in Geophysics
Discussions
Open Access
EGU

133 A similar approach is to replace *u* and *v* with sea surface displacement.

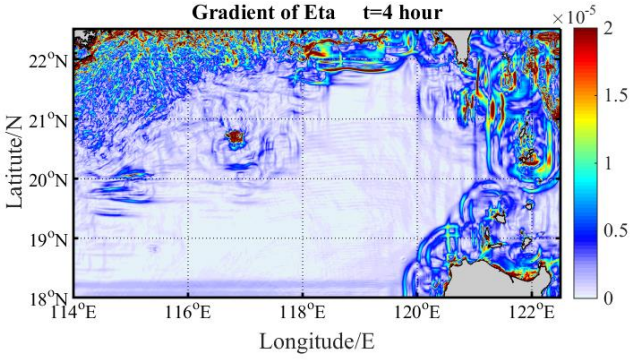

134

135 **Figure 3: Roughness of the sea surface elevation (color contour, unit: 1/s) at 4 hour. Signatures of internal**
136 **waves are found in Luzon Strait, around Dongsha Island and near the northern shelf break.**

137

138 Figure 3 gives gradient of sea surface displacement after 4 hours' simulation. In the northern SCS,
139 internal waves are found in three regions: in Luzon Strait, around the Dongsha Island and near the shelf
140 break. All of the three regions have steep slopes along the tidal current direction, which favors the
141 disturbance of current and therefore the isotherms. The roughness of sea surface over continental shelf
142 is also great, but the active waves there dissipated quickly and no long wave crest is formed.

143 We'll discuss the generation and propagation of internal waves in these three regions.

144 **3.1 Luzon Strait**

145 **3.1.1 In Luzon Strait**

146 Most of the studies on ISWs in the northern SCS indicates that they are generated in Luzon Strait or
147 around (Hsu and Liu, 2000; Zhao et al., 2004; Lien, 2005; Zhang et al., 2005; Fang et al., 2005;
148 Zheng et al., 2008; Du et al., 2008; Warn-Varnas et al., 2010; Pinkel et al., 2012; Hsu, 2000; Cai, 2003;
149 Liu and Hsu, 2004; Yuan et al., 2006). Simulations on internal tides further determined that the
150 primary generation sites are along the Lanyu Ridge and weaker generation along the Hengchun Ridge
151 (Niwa and Hibiya, 2004; Zhang and Fringer, 2006; Jan et al., 2008). It also showed that the Hengchun
152 Ridge have the potential either to reduce the energy of westward propagating internal waves (Chao et
153 al., 2007) or amplify westward propagating waves owing to resonance of the semidiurnal internal tide
154 trapped between the ridges (Buijsman et al., 2010a). Zheng et al. (2008) speculated from SAR images

155 that the west slope of Hengchun Ridge is a high possible source sites for long-crest transbasin ISWs
156 in the northern SCS.

157 In our simulation, disturbance of baroclinic current and the fluctuation of isotherms confirm that
158 Luzon Strait is an important source site of the ISWs over the northern shelf of the SCS. To the west of
159 the strait (around 121^{o}E) the density shows a high horizontal gradient. Current and temperature
160 pattern are disturbed when the tidal current flows over the Hengchun Ridge. Therefore, the ridge
161 around 121^{o}E is a main source site of ISWs over the northern shelf of the SCS.

162 In less than 3 hours after the starting of the simulation, strong current perturbation radiated out
163 from the ridges in Luzon Strait. The perturbation releases both eastward and westward propagating
164 waves. In northern portion of the strait, the westward waves are mainly generated over Hengchun
165 Ridge; in southern portion, the internal waves generate in the water channels between the islands,
166 which are parts of the Lanyu Ridge. Due to the sparsely distributed islands, the internal waves
167 generated in the channels are in forms of ripples rings (Fig. 4a). And they become a wave crest when
168 reaching the Hengchun Ridge. The wave crest (Fig. 4b) parallels to Hengchun Ridge, which is the
169 typical pattern in SAR image (Wang et al., 2010). Comparing the sea surface roughness at section
170 21.6^{o}N (Fig. 4c) and the oscillation of isotherms (Fig. 4d), we find that waves with small half-width in
171 the ocean are always corresponding to peaks of roughness at the sea surface. At those points, the wave
172 current also shows strong convergence (Fig. 4d).

Nonlin. Processes Geophys. Discuss., https://doi.org/10.5194/npg-2017-57
Manuscript under review for journal Nonlin. Processes Geophys.
Discussion started: 9 October 2017

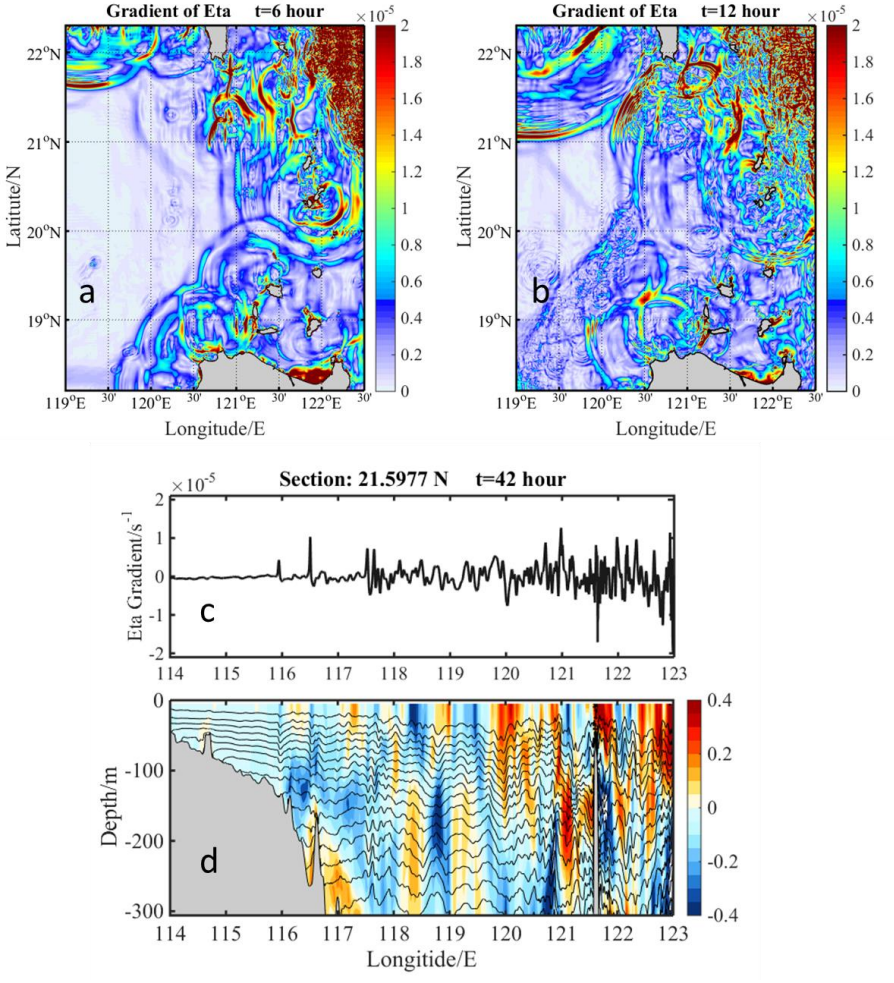

Figure 4: Roughness of sea surface at (a) 6 h and (b) 12 h, (c) at 42 h across 21.6oN section, and (d) the baroclinic current (colored, unit: m/s) and isotherms (black lines) across 21.6oN section.

3.1.2 Diffraction and Interference

Small islands sparsely distributed in the Luzon Strait (see Fig.1c). Between them are shallow water channels, where are the potential source sites of ISWs.

Ebbesmeyer et al. (1991) and Bole et al. (1994) deduced from satellite images that the ISWs in the northern SCS are originated in the 4-km-wide narrow channel between Batan Island and Sabtang Island. Inspecting over 100 SAR images, Hsu et al. (2000) found a crest of ISWs which extend 140 km long

but is only 50 km from those two islands. It indicates that the source site of this wave crest should be extended out of the narrow channel. Tracking back from the propagation direction of the ISWs near Dongsha Island, Cai et al. (2001) inferred that they are generated between Luzon Island and Fuga Island (see Figure 1). Ramp et al. (2012) found ISWs between the ridges just to the south tip of the Taiwan Island, indicating that the origin of ISWs in the northern SCS are not limited in the southern portion of Luzon Strait. Huang et al. (2014) deduced detailed source sites for A waves and B waves: the former is likely generated at the area south of the Batan Island, while the latter is possibly generated at the area south of Itbayat Island and south of the Batan Island.

In our simulation the ripple rings radiate from narrow channels in Luzon Strait (Fig. 4). The widths of these water channels are comparable with the wavelength of internal tides, and they serve as source sites for ISWs. Due to diffraction, the ripple rings extended into the shadows of islands and interference with each other, as the Huyghens' principle states. The longest wave crest in southern portion of Luzon Strait is developed from the ripple rings out of the water channels. When propagating to the Hengchun Ridge, those ripples form a long crest, paralleling to the ridge. Therefore, we cannot deduce the source site of ISWs in Luzon Strait just by tracking back a straight line perpendicular to the wave crest.

For most of the simulation on the internal waves in Luzon Strait, the meridional grids are often compromised to a resolution no less than 1 km to save the computing resource. In narrow channels they are not fine enough to describe diffraction, and then may fail to characterize the long crest near the strait.

3.2 Around Dongsha Island

Nonlinear internal waves around Dongsha Island are found in less than 4 hours after the starting of simulation. Since Dongsha Island is more than 600 km away from the boundary, it is not likely that these nonlinear internal waves are generated in Luzon Strait first and then propagated here in such a short period. Therefore, barotropic tides with speed O(100 m/s) is the possible generator of those waves.

Nonlin. Processes Geophys. Discuss., https://doi.org/10.5194/npg-2017-57
Manuscript under review for journal Nonlin. Processes Geophys.
Discussion started: 9 October 2017

209 **3.2.1 Reflection, diffraction, and interference**

210 In the gradient of sea surface elevation, ripple rings of reflected waves were found propagating
211 away from the Dongsha Island. The amplitude of these waves is about 30 m near the island (Fig. 5).

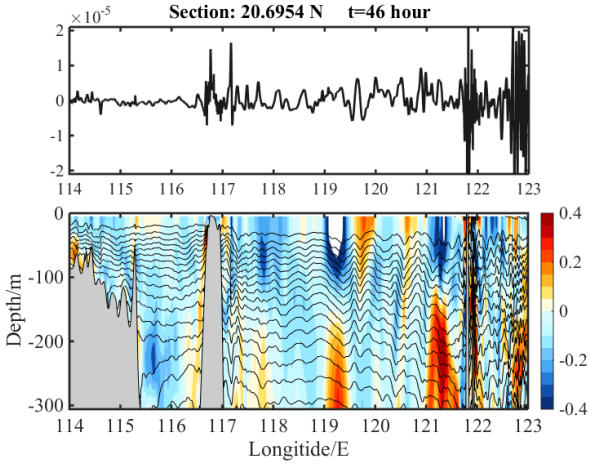

212
213 **Figure 5: Roughness of sea surface at 46 h across 20.7oN section (upper panel), the baroclinic current**
214 **(colored, unit: m/s) and isotherms (black lines) across that section.**

215

216 Due to the small size of Dongsha Island, diffraction of westward ISWs occurred around it. Waves
217 come into the western shadow part of the island after diffracted from north and south tips, and
218 interference take place behind the island. Figure 6 gives four snapshots of a long wave crest meeting
219 the Dongsha Island. At 36 h (Fig. 6a), two long wave crests propagate approaching the east boundary
220 of Dongsha Island. Wave crests are separated by the island into two branches (Fig. 6b). Reflection is
221 also happened but the eastward signal is very weak. With phase speed of about 1.3 m/s, these waves
222 diffract around the island (Fig. 3c). In a semi-diurnal cycle, another crest propagate approaching the
223 island (Fig. 3d).

Nonlin. Processes Geophys. Discuss., https://doi.org/10.5194/npg-2017-57
Manuscript under review for journal Nonlin. Processes Geophys.
Discussion started: 9 October 2017

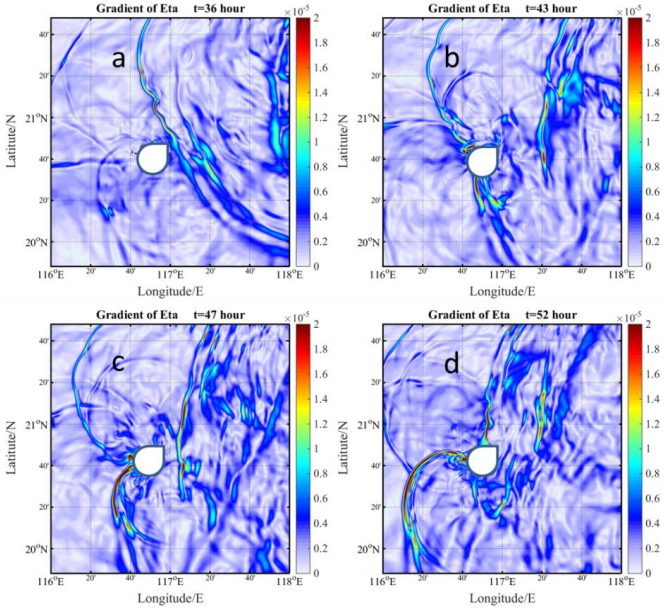

Figure 6: Roughness of the sea surface elevation (color contour, unit: 1/s) near Dongsha Island at four snapshots, (a) 36 h, (b) 43 h, (c) 47 h, and (d) 52 h.

3.2.2 A wave and B wave

Duda et al. (2004) classified the ISWs near Dongsha Island into two categories: A waves (type-a packet, which have one initial large wave and arrives the observation site at roughly the same time in each day), and B waves (type-b packets, which are less regular in amplitudes and wave timing, and arrive Dongsha Island at 25 to 26 hours interval). Zhao et al., (2004) also found internal wave packets in SAR images of two different types: a single-wave ISW packet containing only one ISW with/without an oscillating tail, and a multiple-wave ISW packet composed of a group of rank-ordered ISWs.

Nonlin. Processes Geophys. Discuss., https://doi.org/10.5194/npg-2017-57
Manuscript under review for journal Nonlin. Processes Geophys.
Discussion started: 9 October 2017

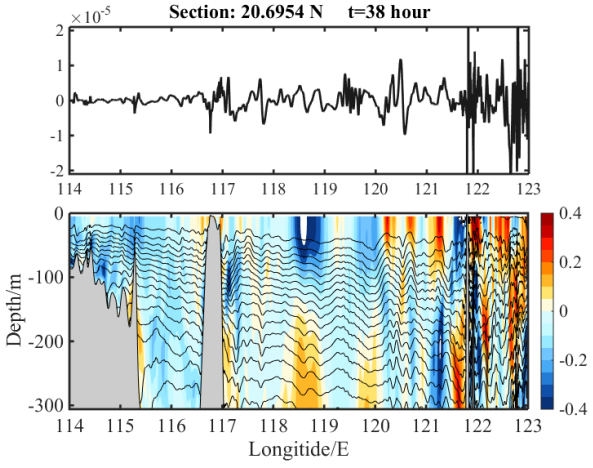

Figure 7: The baroclinic current (colored, unit: m/s) and isotherms (black lines) across 20.7oN section,at 38 h and 44 h, respectively.

The propagation of A waves and B waves could reach a speed about 323 cm/s in the deep basin and 222 cm/s over the continental slope (Ramp et al. 2010). Calculating from a theoretical model, Alford et al. (2010) discussed that A waves travel 5%–10% faster than B waves before they reach the continental slope, while B waves travel 8%–12% faster than A waves on the upper continental slope.

Using the SUNTANS model of a nonhydrostatic simulation, Zhang et al. (2011) discussed that A and B waves arise from the steepening of semidiurnal internal tides that are generated due to strong barotropic flow over ridges in Luzon Strait. A wave is stronger in the southern portion of the Luzon

Nonlin. Processes Geophys. Discuss., https://doi.org/10.5194/npg-2017-57
Manuscript under review for journal Nonlin. Processes Geophys.
Discussion started: 9 October 2017

Strait because diurnal internal tidal beams enhanced the amplitude of the semidiurnal A waves. B wave is stronger in the northern portion where the distance between the two ridges in the strait fits for semidiurnal internal tidal resonance. The orientation of the ridges produces large A waves that propagate into the southern portion of the western SCS basin and stronger B waves that propagate into the northern portion. In Cai et al. (2012), A waves were generated around the time of the spring tides in Luzon Strait and on the strong side of the diurnal inequality, while B waves were generated on the weak side of the diurnal inequality. Note that Zhang et al. (2011) thought B wave is generated by semidiurnal tides while Cai et al. (2012) believed it being generated by diurnal tides, the generation mechanism for B waves is still in doubt. From the SAR images between 1995 and 2001, Zheng (2007) found that only about 22% of ISWs in northern SCS occurred east to 118°E. They are all single-wave ISW packet containing only one ISW (Zhao 2004). Zhao (2004) suspected that some of the ISWs in the northern SCS may not be generated in Luzon Strait, but locally generated in the thermocline by the nonlinear interaction of internal tide beams from at about 120°E.

The observation from October 2010 to September 2011 at center part (119°51'E, 20°33'N) of Luzon Strait seems support that A waves and B waves are from different sources. In the observation lasted almost one year, 105 solitary waves are recorded; all of them are B waves (Li et al., 2014).

Fig. 6 shows two wave crests reach the Dongsha Island at about semi-diurnal period. They are originated from different sites. The first crest generated at the northern shelf of the SCS, while the second crest generated in Luzon Strait. It is possible that A waves or B waves are not generated in Luzon Strait but near the continental shelf break.

3.3 Near Continental shelf break

In statistics of ISWs imaged by SAR (e.g., Zhao et al., 2004; Zheng et al., 2007; Gan et al., 2007; Yang et al., 2009), the wave crests to the west of 120°E distributed much denser than to the east, and even more denser to the west of 118°E. For example, from the SAR images between 1995 and 2001, Zheng (2007) found that only about 22% of ISWs in northern SCS occurred east to 118°E.

Yang et al., (2004) believed that ISWs can be generated around shelf break by internal tide. Duda et al. (2004) found that there are two categories of transbasin ISWs in the northern SCS: generated in the Luzon Strait by tide or Kuroshio current, or generated at or near the continental shelf break by

transbasin waves and/or the diurnal tide.

When internal waves in Luzon Strait propagate westward into the SCS, increasing of nonlinear effect enforces them into ISWs. During their way up to the shelf slope, due to the westward shoaling of thermocline, their phase speed slows down. Therefore, there are more ISWs in shower regions. Another reason for the non-homogenous distribution of wave crests is that some ISWs are generated just over the slope by barotropic tides.

Besides the internal waves generated in Luzon Strait, internal waves near the shelf break also become discernable no later than four hours after the starting of the simulation. Our simulation found that the ISWs leave the Luzon Strait at about one diurnal cycle. Those waves found near the continental shelf break seem not related to those internal waves generated in the Luzon Strait. In fact, only barotropic wave (tidal current) is fast enough to cover four arc degrees in four hours. That is to see, the internal waves near the shelf break is more likely being generated by barotropic tide rather than internal tide.

3.3.1 Source sites near the shelf break

Simulation shows that internal waves generated over the slope form ripple rings and propagate leaving the source site. The most prominent sea surface gradient is found about 2 degrees west to the south tip of Taiwan Island (Fig. 7a). And another one is found south-east to the Hainan Island (Fig. 7b).

Nonlin. Processes Geophys. Discuss., https://doi.org/10.5194/npg-2017-57
Manuscript under review for journal Nonlin. Processes Geophys.
Discussion started: 9 October 2017

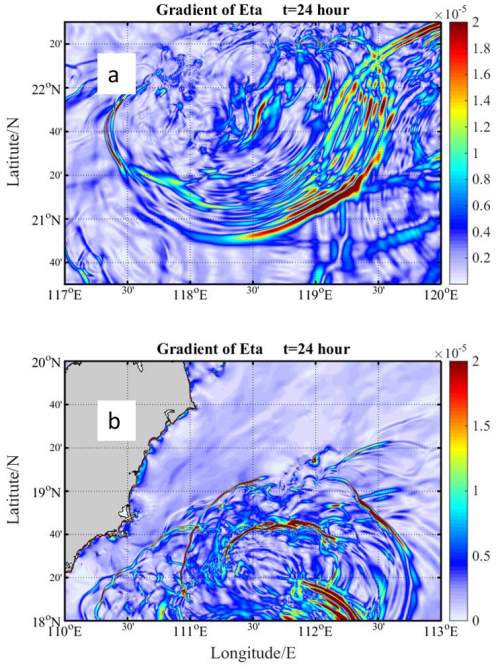

Figure 7: Roughness of the sea surface (color contour, unit: 1/s) near northern continual shelf of SCS (a) west to the south tip of Taiwan Island and (b) south-east to the Hainan Island.

Non-uniformity of the model's initial state is not necessary for the generation of internal waves near the shelf. In another simulation started from uniformly initial state, we also find internal waves generated several hours from the starting of the simulation.

3.3.2 Shape of the ISWs

In the simulation, both depression and elevation ISWs are found near the shelf break. We also find a snapshot when the isotherms in upper layers show elevation while those in deep layers are depression (Fig. 8). It is a typical mode two ISW, which is not often found in the SCS. In the previous studies, mode two ISWs had even been found at about 117°E in a zonal section (Yang, 2009) and between the ridges just to the south tip of the Taiwan Island (Ramp et al., 2012).

The largest amplitude of ISWs is commonly found near the pycnocline. In our simulation, however, the ISWs near the shelf break reach their largest amplitude near the bottom (at about 200-m depth). The

Nonlin. Processes Geophys. Discuss., https://doi.org/10.5194/npg-2017-57
Manuscript under review for journal Nonlin. Processes Geophys.
Discussion started: 9 October 2017

corresponding baroclinic current implies that the ISWs in this region are mode two ISWs. Amplitude of the mode two ISWs reach maximums on both sides of the pycnocline.

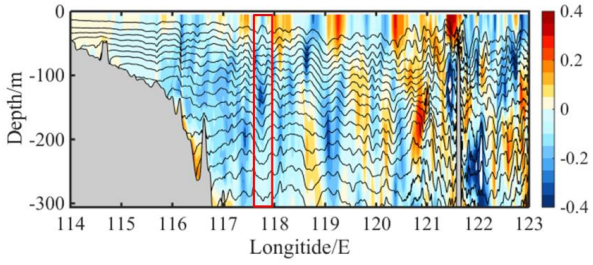

Figure 8: The baroclinic current (colored, unit: m/s) and isotherms (black lines) across 21.6oN section, at 50 h.

The internal waves fission over the shelf into several packets. Therefore, we find a big depression wave followed by a pack of A waves over the slope, as Fig. 9 shows.

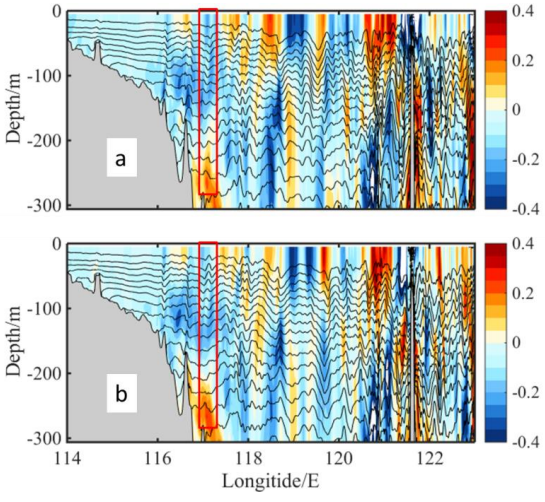

Figure 9: The baroclinic current (colored, unit: m/s) and isotherms (black lines) across 21.6°N section, at (a) 36 h, and (b) 38 h.

4. Conclusion

We set up a non-hydrostatic MITgcm model to study the generation of ISWs in the northern SCS in non-uniformly initial temperature/salinity fields. In the simulations, the propagation of the ISWs across

the SCS is similar to the schematic figure illustrated by Simmons et al. (2011). Our simulation, however, reveals detailed source sites and evolution of ISWs. We find that the source sites of the ISWs in the northern SCS are not limited in Luzon Strait. The shelf break and Dongsha Island are also important source sites. And, the ISWs generated in these sites are likely being excited by barotropic tide current from the Pacific rather than by internal tides.

In south portion of Luzon Strait, the internal waves generated and propagated out in the form of ripple rings. Those rings form a long crest when they reach the Hengchun Ridge.

Simulation find that the wave crests near Dongsha Island comes from two areas: the northern shelf break and Luzon Strait. A waves and B waves often observed near Dongsha Island may come from these two areas, respectively.

Previous studies use the horizontal uniformly stratification as the initial state of numerical simulation. It is reasonable when study the generation mechanism of the internal waves, but may have some deficiency in practice. Firstly, it will take the model a longer time to reach the state as that of the real ocean. Therefore, it is difficult to compare the simulation with real-time observations. Secondly, the horizontal uniformly stratification comes from one profile of temperature and salinity, which is often taken from deep-water region. Considering the westward shoaling of the stratification in the SCS, the deviation caused by the stratification bias is expected. We believe that start the simulation from non-uniformly stratification will reduce the possible bias caused by the westward shoaling thermocline in the SCS and shorten the time for the model to get a steady state. Therefore, the simulation is likely to yield internal waves more similar to the observations, and is thus applicable for the prediction of internal waves in the SCS.

Acknowledgments G. Wang is supported by the National Key Research and Development Program of China grant nos. 2016YFC1401407 and 2016YFB0201100, the National Natural Science Foundation of China under grant no. 41476024; F. Qiao, D. Dai and Y. Zhang are supported by the NSFC-Shandong Joint Fund for Marine Science Research Centers of China grant no. U1406404 and the International Cooperation Project of Indo-Pacific Ocean Environment Variation and Air-Sea Interaction of contract no. GASI-03-IPOVAI-05.

References

Alford, M. H., Lien, R. C. , Simmons, H., et al: Speed and evolution of nonlinear internal waves transiting the South China Sea, J. Phys. Oceanogr., 40, 1338–1355, 2010.

Alfort, M. H., Peacock, T., MacKinnon, J. A., et al: The formation and fate of internal waves in the South China Sea, Nature 521, 65–69, doi:10.1038/nature14399, 2015.

Alper, W.: Theory of radar imaging of internal waves, Nature, 34(6008), 245–247, 1985.

Amante, C., and Eakins, B. W.: ETOPO1 1 arc-minute global relief model: procedures, data sources and analysis, NAOO Technical Memorandum NESDIS NGDC-24, National Geophysical Data Center, NOAA, doi:10.7289/V4C8276M, 2009.

Buijsman, M. C., McWilliams, J. C., and Jackson, C. R.: East-west asymmetry in nonlinear internal waves from Luzon Strait, J. Geophys. Res., 115, C10057, doi:10.1029/2009JC006004, 2010.

Buijsman, M. C., Kanarska, Y., and McWilliams, J. C.: On the generation and evolution of nonlinear internal waves in the South China Sea, J. Geophys. Res., 115, C02012, doi:10.1029/2009JC005275, 2010.

Buijsman, M. C., Legg, S., and Klymak, J. M.: Double-ridge internal tide interference and its effect on dissipation in Luzon Strait, J. Phys. Oceanogr., 42, 1337–1356, doi:10.1175/JPO-D-11-0210.1, 2012.

Buijsman, M. C., Klymak, J. M., Legg, S., et al: Three-dimensional double-ridge internal tide resonance in Luzon Strait, J. Phys. Oceanogr. 44, 850–869, doi:10.1175/JPO-D-13-024.1, 2014.

Cai, S., Gan, Z., and Long, X.: Some characteristics and evolutions ofthe internal solitary waves in the northern South China Sea, Science Bulletin (Chin) , 46(15), 1245–1230, 2001.

Cai, S., Long, X., and Gan, Z.: A numerical study of the generation and propagation of internal solitary waves in the Luzon Strait, Oceanologica Acta, 25(2), 51–60, 2002.

Cai, S., Long, X., Huang, Q.: Preliminary numerical study on the generation condition of induced internal solitons in the northern South China Sea, Acta Oceanol. Sin., 25(4), 119–124, 2003.

Cai, S., Xie, J., and He, J.: An overview of internal solitary waves in the South China Sea. Surveys in Geophysics, 33(5), 927–943, 2012.

Cai, S., Xie, J., Xu, J., et al: Monthly variation of some parameters about internal solitary waves in the South China Sea, Deep-Sea Res., I 84, 73–85, 2014.

379 Chao, S. Y., Ko, D. S., Lien, R. C., et al: Assessing the west ridge of Luzon Strait as an internal wave
380 mediator, J. Oceanogr.,.63, 897–911, 2007.
381 Du, T., Tseng, Y. H., and Yan, X. H.: Impacts of tidal currents and Kuroshio intrusion on the generation
382 of nonlinear internal waves in Luzon Strait, J. Geophys. Res., l13, C08015,
383 doi:10.1029/20O7JC004294, 2008.
384 Duda, T. F., Lynch, J. F., Irish, J. D., et al: Internal tide and nonlinear internal wave behavior at the
385 continental slope in the northern South China Sea, IEEE J. Ocean Eng. 29(4), 1105–1130, 2004.
386 Dong, J., Zhao, W., Chen, H., et al: Asymmetry of internal waves and its effcts on the ecological
387 environmentg observed in the northern South China Sea, Deep-Sea Res. I, 98, 94–101, 2015.
388 Egbert, G. D., and Erofeeva, S. Y: Efficient inverse modeling of barotropic ocean tides, J. Atmos
389 Oceanic Technol., 19(2), 183-204, 2002.
390 Fang, W., Shi, P., Long, X., et al: In situ observation of internal solitaries in north of South China Sea.
391 Chin. Sci. Bull. (Chinese), 50, 1400–1404, 2005.
392 Fang, X. H., and Du, T.: Fundamental of ocean internal waves and internal waves in China Seas
393 (Chinese), Qingdao, Press of Ocean University of China, 2005.
394 Farmer, D., Li, Q., and Park, J.: Internal wave observations in the South China Sea: the role of ratation
395 and nonlinearity, Atmosphere-Ocean, 47(4), 267–280, 2009.
396 Gan, X., Huang, W., Yang, J., et al: The study of spatial and temporal distribution characteristics of
397 internal waves in the South China Sea from multi-satellite data. Remote Sensing Technology and
398 Application (Chinese), 22(2), 242–246, 2007.
399 Gao, Kun., Chen, X., Yu, H., et al: The influence of internal tide on the diagnostic calculation of
400 geostrophic current in Luzon Strait, Periodical of Ocean University of China (Chinese), 40(2), 9–
401 16, 2010.
402 Guo, C., Chen, X., Vlasenko, V., et al: Numerical investigation of internal solitary waves from the
403 Luzon Strait: generation process, mechanism and three-dimensional effects, Ocean Modell., 38,
404 203–216,2011.
405 Guo, C., and Chen, X.: Numerical investigation of large amplitude second mode internal solitary waves
406 over a slope-shelf topography, Ocean Modell., 42, 80–91, 2012.
407 Guo, C,. Vlasenko, V., Alpers, W., et al: Evidence of short internal waves trailing strong internal
408 solitary waves in the northern South China Sea from synthetic aperture radar observations,

Romote Sensing of Evironment, 124, 542–550, 2012.

Hsu, M. K., and Liu, A. K.: Nonlinear internal waves in the South China Sea, Can. J. Remote Sens., 26, 72–81, 2000.

Huang, X., Zhao, W., Tian, J., et al: Mooring observations of internal solitary waves in the deep basin west of Luzon Strait, Acta Oceanol. Sin., 33(3), 82–89, doi:10.1007/s13131-014-0416-7, 2014.

Jan, S., Chern, C. S., Wang, J., et al: Generation of diurnal K1 internal tide in the Luzon Strait and its influence on surface tide in the South China Sea, J. Geophys. Res., 112, C06019, doi:10.1029/2006JC004003, 2007.

Jan, S., Lien, R. C., and Ting, C. H: Numerical study of baroclinic tides in Luzon Strait, J. Oceanogr. 64, 789–802, 2008.

Jan, S., Chern, C. S., Wang, J., et al: Generation and propagation of baroclinic tides modified by the Kuroshio in the Luzon Strait, J. Geophys. Res., 117, C02019. doi:10.1029/2011JC007229, 2012.

Klymak, J. M., Pinkel, R., Liu, C. T., et al: Prototypical solitons in the South China Sea, Geophys. Res. Lett., 33, L11607, doi:10.1029/2006GL025932, 2006.

Li, D., Chen, X., and Liu, A.: On the generation and evolution of internal solitary waves in the northwestern South China Sea, Ocean Modell., 40, 105–119 , 2011.

Li, H., Song, D., Chen, X., et al: Numerical study of M2 internal tide generation and propagation in the Luzon Strait, Acta Oceanol. Sin., 30(5), 23–32, 2011.

Li, M., Hou, Y., Li, Y., et al: Energetics and temporal variability of internal tides in Luzon Strait: a nonhydrostatic numerical simulation, Chin. J. Oceanol. Limmol. 30(5), 852–867, 2012.

Li, Q., and Farmer, D. M.: The generation and evolution of nonlinear internal waves in the deep basin of the South China Sea. J Geophys Res 41:1345–1363, 2011.

Li Z, Cai S, Chen J et al (2014) Preliminary analysis of observations by deep submersible mooring in west Luzon Strait during 2010 to 2011. Journal of Tropical Oceanography (Chin) 33(1):10–16

Liao, G., Yuan, Y., Arata, K., et al: Analysis of internal tidal characteristics in the layer above 450 m from acoustic Doppler current profiler observations in the Luzon Strait, Science China Earth Sciences, 54(7), 1078–1094, 2011.

Lien, R. C., Tang, T. Y., Chang, M. H., et al: Energy of nonlinear int ernal waves in the South China Sea, Geophys, Res, Lett, 32, L05615. doi:10.1029/2004GL022012, 2005.

Liu, A. K., and Hsu, M. K.: Internal wave study in the South China Sea using Synthetic Aperture Radar

(SAR), INT. J. Remote Sensing, 25, 1261–1274, 2004.

Liu, A. K., and Hsu, M. K. Satellite remote sensing of nonlinear internal waves in the South China Sea, Proceedings of the Third International Deep Ocean Technology Symposium Beijing, China, June 28-July 1, 2009.

Locarnini, R. A., Mishonov, A. V., Antonov, J. I., et al: World Ocean Atlas 2013, Volume 1: Temperature. S. Levitus, Ed., A. Mishonov Technical Ed.; NOAA Atlas NESDIS, 73, 40pp, 2013.

Marshall, J., Adcroft, A., Hill, C., Perelman, L., and Heisey, C.: A finite-volume, incompressible Navier Stokes model for studies of the ocean on parallel computers, J. Geograph. Res., 102(C3), 5753-5766, doi: 10.1029/96JC02775, 1997.

Orr, M. H., and Mignerey, P. C.: Nonlinear internal waves in the South China Sea: observation of the conversion of depression internal waves to elevation internal waves, J. Geophys. Res. 108(C3), 3064, doi:10.1029/2001JC001163, 2003.

Pickering, A., Alford, M. H., Buijsman, M. C., et al: Structure and variability of internal tides in Luzon Strait, J. Phys. Oceanogr., 45(6), 150402094400007, doi:10.1175/JPO-D-14-0250, 2015.

Pinkel, R., Muijsman, M., and Klymak, J. M.: Breaking topographic lee waves in a tidal channel in Luzon Strait, Oceanography, 25(2), 160–165, 2012.

Rainville, L., Lee, C. M., Rudnick, D. L., et al: Propagation of internal tides generated near Luzon Strait: observations from autonomous gliders, J. Geophys. Res.: Oceans, 118, 4125–4138, doi:10.1002/jgrc.20293, 2013.

Ramp, S. R., Tang, T. Y., Duda, T. F., et al: Internal solitons in the northeastern South China Sea, Part I: sources and deep water propagation, IEEE J. Ocean Eng., 29(4), 1157–1181, 2004.

Si, G., Hou, Y., Qi, P., et al: Characteristics of nonlinear internal waves observed in the northern South China Sea, Chin. J. Oceanol. Limnol ., 28(5), 1068–1072, 2010.

Simmons, H., Chang, M. H., Chang, Y. T., et al: Modeling and prediction of internal waves in the South China Sea, Oceanography, 24(4), 88–99, http://dx.doi.org/10.5670/oceanog.2011.97, 2011.

Smith, W. H. F., and Sandwell, D. T.: Global sea floor topography from satellite altimetry and ship depth soundings, Science, 277, 1956–1962, 1997.

Song, D., Pohlmann, T., Chen, X., et al: The role of sea water viscidity in modeling the vertical movement of internal tides, Ocean Modell., 34, 63–69, 2010.

469 Sun, Z., Hu, J., Zheng, Q., et al: Comparison of typhoon-induced near-inertial oscillations in shear flow
470 in the northern South China Sea, Acta Oceanol. Sin., 34(11), 38–45, 2015.
471 Tian, J., Yang, Q., Liang, X., et al: Observation of Luzon Strait transport, Geophys. Res. Lett. 33,
472 L19607, 2006.
473 Vlasenko, V., Stashchuk, N., Guo, C., et al: Multimodal structure of baroclinic tides in the South China
474 Sea, Nonlin. Processes Geophys., 17, 529–543, doi: 10.5194/npg-17-529-2010, 2010.
475 Vlasenko, V., Guo, C., and Stashchuk, N.: On the mechanism of A-type and B-type internal solitary
476 waves in the northern South China Sea, Deep-Sea Res. I, 69:100–112, 2012.
477 Wang, D. P.: Diurnal modulation of semidiurnal internal tides in Luzon Strait, Ocean Modell., 59-60,
478 1–10, 2012.
479 Wang, G., Qiao, F., and Dai, D.: A 2D-numerical modeling of the generation and propagation of
480 internal solitary waves in the Luzon Strait, Acta Oceanol. Sin., 29(6), 1–11, 2010.
481 Wang, G., Zheng, Q., Lin, M., et al: Three dimensional simulations of internal wave attractors in the
482 Luzon Strait, Acta Oceanol. Sin., 34(11), 14–21. doi:10.1007/s13131-015-0477-2, 2015.
483 Wang, X., Peng, S., Liu, Z., et al: Tidal mixing in the South China Sea: an estimate based on the
484 internal tide energetics, J. Phys. Oceanogr., 46, 107–124, doi:10.1175/JPO-D-15-0082.1, 2016.
485 Warn-Varnas, A., Hawkins, J., Lamb, K. G., et al: Solitary wave generation dynamics at Luzon Strait,
486 Ocean Modell., 31(1-2), 9-27, doi:10.1016/j.Ocemod.2009.08.002. , 2010.
487 Xu, Z., Yin, B., Hou, Y., et al: A study of internal solitary waves observed on the continental shelf in
488 the northwestern South China Sea, Acta Oceanol. Sin., 29(3), 18–25, 2010a.
489 Xu, Z., Yin, B., and Hou, Y.: Highly nonlinear internal waves over the continental shelf of the
490 northwestern South China Sea, Chin. J. Oceanol. Limnol., 28(5), 1049–1054, 2010b.
491 Yang, J. S., Xiao, Q. M., Huang, W. G., et al: Nonlinear ocean internal waves Observed by
492 multifrequency synthetic aperture radar, Acta Oceanol. Sin., 27(Supp), 151–154, 2008.
493 Yang, Y. J., Tang, T. Y., Chang, M. H., et al: Solitons Northeast of Tung-Sha Island during the ASIAEX
494 pilot studies, IEEE J. Ocean Eng. 29(4), 1182–1199, 2004.
495 Yang, Y. J., Chang, M. H., Tang, T. Y.: Observations of second baroclinic mode internal solitary waves
496 on the continental slope of the northern South China Sea, J. Geophys. Res., 114, C10003,
497 doi:10.1029/2009JC005318, 2009.
498 Yuan, Y., Zheng, Q., Dai, D., et al: Mechanism of internai waves in the Luzon Strait, J. Ceophys. Res.

111, C1IS17, doi:10.1029/2005JC0O3198, 2006.

Zhang, X., Liang, X., and Tian, J.: Study On the internal tide and near-inertial movement in the upper 450 meters in the northern SCS, Chin. Sci. Bull., 50(18), 2027–2031, 2005.

Zhang, Z., Fringer, O. B., and Ramp, S. R.: Three-dimensional nonhydrostatic numerical simulation of nonlinear internal wave generation and propagation in the South China Sea, J. Geophys. Res., 116, C05022, doi:10.1029/2010JC006424, 2011.

Zhao, Z., Klemas, V., Zheng, Q., et al: Remote sensing evidence for baroclinic tide origin of internal solitary waves in the northeastern South China Sea, Geophys. Res. Lett., 31, L06302, doi:10.1029/2003G1019077, 2004.

Zhao, Z.: Internal tide radiation from the Luzon Strait, J. Geophys. Res.: Oceans, 119, 5434–5448, doi:10.1002/2014JC010014, 2014.

Zheng, Q., Susanto, R. D., Ho, C. R., et al: Statistical and dynamical analyses of generation mechanisms of solitary internal waves in the northern South China Sea, J. Geophys. Res. 112, C03021, doi:1029/2006JC003551, 2007.

Zheng, Q., Tony, S. Y., Lin, H., et al: On generation source sites of internal waves in the Luzon Strait. Acta Oceanol. Sin., 27(3), 38–50, 2008.

Zweng, M. M., Reagan, J. R., Antonov, J. I., et al: World Ocean Atlas 2013, Volume 2: Salinity, S. Levitus, Ed., A. Mishonov Technical Ed.; NOAA Atlas NESDIS 74, 39pp, 2013.